DOI: 10.1002/ejic.200501114

Study of Thermodynamic and Kinetic Stability of Transition Metal and Lanthanide Complexes of DTPA Analogues with a Phosphorus Acid Pendant Arm

Jan Kotek,*[a,c] Ferenc K. Kálmán,[b] Petr Hermann,[a] Ernő Brücher,[b] Koen Binnemans,[c] and Ivan Lukeš[a]

Keywords: Phosphonate complexes / Phosphinate complexes / MRI contrast agents / Kinetics / Thermodynamics

The thermodynamic and kinetic stabilities of the complexes of phosphonate and phenylphosphinate analogues of H_5dtpa with selected transition- and lanthanide-metal ions are presented. Both phosphorus-containing ligands form thermodynamically very stable complexes, with stability constants comparable with or even higher than those reported for the parent H_5dtpa. However, the kinetic inertness of their gadolinium(III) complexes against acid- and metal-assisted decomplexations is surprisingly much lower. The half-life times of gadolinium(III) complexes of the new ligands in the presence of excess of concurrent metal ions [copper(II) or europium(III)] are about 2–3 orders of magnitude shorter compared to H_5dtpa and its amide derivatives. The behaviour can probably be attributed to steric strain in the new complexes, to the high affinity of phosphonate ligand for proton, and/or to easy formation of binuclear complexes, which act as intermediates in the complex dissociation.

Introduction

Multidentate ligands and their complexes are frequently used in medicine. Gadolinium(III) complexes of octadentate ligands having the ninth coordination site occupied with a water molecule are utilized as contrast agents (CA) in magnetic resonance imaging (MRI).[1–3] As such toxic-metal-containing contrast agents have to be administered in relatively high doses, the gadolinium(III) ion must be encapsulated in stable complexes. These must survive with no decomplexation in body fluids containing many concurrent ligands (amino acids, phosphate anion, peptides etc.) and metal ions (e.g. Ca^{2+}, Zn^{2+}, Cu^{2+}). Ligands whose complexes fulfil such stability requirements are mostly derivatives of two prototype ligands (Scheme 1) – macrocyclic 1,4,7,10-tetraazacyclododecane-1,4,7,10-tetraacetic acid (H_4dota) and acyclic diethylenetriaminepentaacetic acid (H_5dtpa, 1,4,7-triazaheptane-1,1,4,7,7-pentaacetic acid). In vivo stability of the complexes may be estimated from thermodynamic and kinetic properties. The thermodynamic stability of metal complexes of H_5dtpa and H_4dota (expressed as stability constants) is very high. Ligands derived from the linear ligand H_5dtpa are in general much cheaper and more easily available than derivatives of the macrocyclic H_4dota. However, the resistance of complexes of macrocyclic ligands against decomplexation in body fluids (measured e.g. as acid- or metal-assisted dissociations) is usually much higher.[4,5]

According to theory, the water molecule which saturates the coordination sphere of the central Gd^{3+} ion should be bound in the complex for an optimal residence time before exchange with bulk water. The residence time should lay in the range of 20–30 ns for MRI contrast agents used at magnetic fields applied in commercial tomographs, and in addition, the molecular tumbling of the CA should be as slow as possible.[1–3,6] However, the complexes of H_4dota and H_5dtpa themselves are far from such optimum.[7] In the search for better MRI contrast agents, sterically crowded ligands were developed as the enhanced steric strain around metal-binding site increases the exchange rate of coordinated water molecule. The steric strain was usually reached by introduction of one extra methylene group into the backbone (propylene group instead of ethylene bridge) or in one of the pendant arms (i.e. with propionate pendant instead of acetate),[8–11] or by substitution of ligand backbone by alkyl/aryl group.[12,13] The complexes formed with these new ligands are thermodynamically usually slightly less stable than those of H_4dota and H_5dtpa.[9,10,14,15] Unfortunately, no detailed kinetic studies are available in the literature for these complexes.

[a] Department of Inorganic Chemistry, Charles University, Hlavova 2030, 128 40 Prague 2, Czech Republic
[b] Department of Inorganic and Analytical Chemistry, University of Debrecen, 4010 Debrecen, Hungary
[c] Department of Chemistry, Katholieke Universiteit Leuven, Celestijnenlaan 200F, 3001 Leuven, Belgium
E-mail: modrej@natur.cuni.cz
Supporting information for this article is available on the WWW under http://www.eurjic.org or from the author.

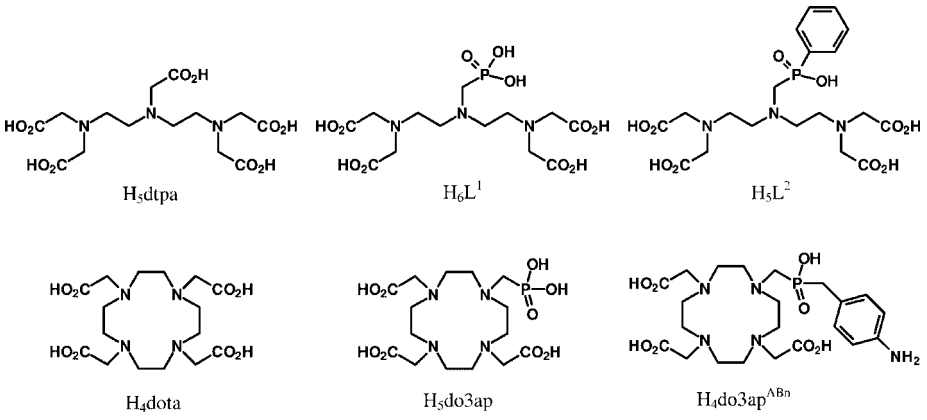

Scheme 1. Structural formulas of the ligands mentioned in the text.

To contribute to this field, we prepared several analogues of H_4dota and H_5dtpa having a bulkier phosphorus acid pendant moiety instead of the carboxylate group. The corresponding lanthanide(III) complexes of the linear ligands H_6L^1 and H_5L^2 (Scheme 1) have been studied by NMR and relaxometry.[16] It was shown, that the water-exchange rate is much higher for the complexes with phosphorus-containing ligands than what was reported for the complexes of H_5dtpa and its amides. Noticeable acceleration of water exchange was observed also for macrocyclic ligands with one phosphorus-based pendant arm (e.g. H_5do3ap or H_4do3ap^{ABn}, Scheme 1) comparing to H_4dota.[17,18] Furthermore, the relatively easy substitution on the phosphorus atom offers the possibility to attach the complex to a macromolecular carrier,[19–21] or to bind it non-covalently to plasma proteins (e.g. by hydrophobic interactions).[16] Here we report on the thermodynamic and kinetic stability studies of the complexes of two linear ligands – phosphonate and phenylphosphinate derivatives H_6L^1 and H_5L^2, respectively (Scheme 1) – with selected divalent transition and trivalent lanthanide metal ions.

Results and Discussion

Crystal Structure of $H_6L^1 \cdot HCl \cdot 1.5H_2O$

In the crystal structure, a molecule of the ligand is present in the charged sevenfold-protonated form $(H_7L^1)^+$ (Figure 1). All the nitrogen atoms of the backbone are protonated together with one oxygen atom of the phosphonate moiety (O1) and three carboxylate oxygen atoms (O111, O211 and O311). The geometry around the phosphorus atom is tetrahedral, with noticeably longer P–O bond to the protonated oxygen O1 comparing to others (Table 1). One chloride anion serves as counterion. Additionally, two water molecules were found in the structure, but one of them (O2W) is best refined with a half-occupancy. Molecules of the ligand are connected by short hydrogen bonds (2.45–

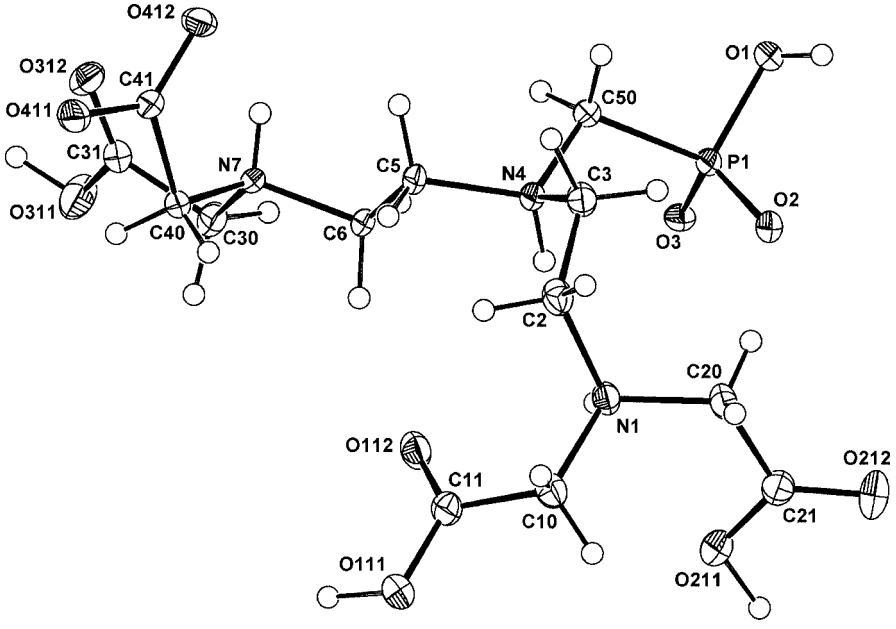

Figure 1. Molecular structure of $(H_7L^1)^+$ with atom numbering scheme.

2.65 Å) between protonated and unprotonated oxygen atoms of acetate and phosphonate moieties. Furthermore, the protonated amino groups are also involved in rather strong (2.64–2.77 Å) hydrogen binding to oxygen atoms of neighbouring ligand molecules. Additionally, the solvate water molecules and chloride anion bind each other (3.04–3.20 Å), and also the water molecule O1W has a short contact to protonated carboxylate oxygen atom O311 (Table S1).

Table 1. Geometry of the phosphonate group in the structure of $H_6L^1 \cdot HCl \cdot 1.5H_2O$.

Distances [Å]		Angles [°]	
P1–O1	1.5740(13)	O1–P1–O2	110.00(8)
P1–O2	1.5038(13)	O1–P1–O3	110.87(7)
P1–O3	1.4977(13)	O2–P1–O3	115.71(7)
P1–C50	1.827(2)	C50–P1–O1	101.94(8)
		C50–P1–O2	109.53(8)
		C50–P1–O3	107.85(9)

Equilibrium Studies

The protonation and complexation equilibrium were studied by conventional potentiometry. Table 2 lists the protonation constants of concerned ligands together with those of H_5dtpa. Distribution diagrams of H_6L^1 and H_5L^2 are shown in Figure S1 (supporting information; for supp. inf. see also the footnote on the first page of this article. As polydentate aminocarboxylic acids can form relatively strong complexes with alkali metal ions, the potentiometric studies were performed using tetramethylammonium chloride (TMAC) as a background electrolyte. Indeed, the determined values of the highest protonation constants are systematically higher than those reported previously,[16] which were obtained by NMR and are lower as a consequence of sodium(I)-induced deprotonation (Table 2). A similar trend was observed also for H_5dtpa, where constant $\log\beta_1$ determined with NaCl as the supporting electrolyte is about one order of magnitude lower (9.45[22]) than that measured in TMAC (10.41,[22] Table 2). Accordingly to NMR-assigned sites of protonations[16] and well-known protonation Scheme of H_5dtpa itself,[23] the first and second protonations take place on the nitrogen atoms of the ligand backbone. In the case of the phosphonate ligand H_6L^1, the third protonation (pK_A = 7.57) corresponds to the protonation of the phosphonate moiety. Other protonations have pK_A's values close to each other and correspond to the carboxylate pendants. Deprotonation of the singly protonated phosphonate ligand $(HL^1)^{5-}$ occurs at very high pH (pK_A = 11.82) comparing to the phosphinate derivative and H_5dtpa (pK_A's 10.28 and 10.41, respectively), as a result of spreading of high electron density of fully deprotonated phosphonate (charge 2–) to the neighbouring nitrogen atom. This trend is usually observed for analogous aminocarboxylic/phosphorus acid derivatives.[24] The potentiometric data of the ligand/metal mixtures were best fitted according to a model employing the formation of 1:1 and 1:2 ligand-to-metal complexes in various protonation states. The resulting stability constants of the complexes are compiled in Tables 3, 4, 5 and 6. In the case of 1:1 complexes with the transition-metal ions Cu^{2+} and Zn^{2+}, all nitrogen atoms of the ligands are probably coordinated to the metal ion, and no free metal ions are present in the mixtures above pH ≈ 2.7. As usual, the coordination number of transition metal ions is 6, and the hapticity of the ligands studied is higher (8), the coordination sphere of the central metal ion is closed by two or three oxygen atoms of the pendant arms and some pendants remain uncoordinated (and can bind another metal ion in binuclear complexes, see below). The protonation of the $[M(L^1)]^{4-}$ species takes place on the phosphonate pendant moiety, which is probably coordinated (corresponding pK_A slightly dropped comparing to the free ligand, 6.86 and 7.24 vs. 7.57, respectively). Other protonations takes place on oxygen atoms of the uncoordinated carboxylates (pK_A's in range 1.37–3.97). Contrary, protonation of calcium(II) complexes takes place on the nitrogen atoms, as the corresponding pK_A's are noticeably higher than that of acetates in the free ligands. In a twofold excess of the metal ion, complexes of M_2L stoichiometry are formed. They loose additional two protons with increasing pH, forming bis(hydroxo) species. Because the corresponding dissociation constants are similar for both stepwise deprotonations [9.39 and 7.74 for copper(II) and 8.81 and 8.86 for zinc(II) complexes, respectively], these deprotonations occur almost simultaneously. The stability constant of the dinuclear species is lower, but still comparable to that of iminodiacetic acid, so the coordination of each

Table 2. Protonation constants $\log\beta_h$[a] of H_6L^1, H_5L^2 and H_5dtpa and corresponding dissociation constants $pK_{A,h}$[a] (I = 0.1 M NMe_4Cl, 25 °C, unless stated otherwise).

Constant	H_6L^1 present work		ref.[16][b]		H_5L^2 present work		ref.[16][b]		H_5dtpa ref.[22]	
	$\log\beta_h$	$pK_{A,h}$	$\log\beta_h$	$pK_{A,h}$	$\log\beta_h$	$pK_{A,h}$	$\log\beta_h$	$pK_{A,h}$	$\log\beta_h$	$pK_{A,h}$
$\log\beta_1$	11.82(8)	11.82	10.75	10.75	10.28(1)	10.28	9.60	9.60	10.41	10.41
$\log\beta_2$	20.12(5)	8.30	18.63	7.88	19.29(1)	9.01	18.7	9.10	18.78	8.37
$\log\beta_3$	27.69(3)	7.57	25.55	6.92	22.46(2)	3.17	21.33	2.63	22.87	4.09
$\log\beta_4$	30.78(7)	3.09	28.25	2.70	24.82(2)	2.36	23.48	2.15	25.38	2.51
$\log\beta_5$	33.33(5)	2.55	30.42	2.17	26.97(2)	2.15	–	–	27.42	2.04
$\log\beta_6$	35.23(8)	1.90	–	–	–	–	–	–	–	–
$\log\beta_7$	36.44(9)	1.21	–	–	–	–	–	–	–	–

[a] $\beta_h = [H_hL]/([H]^h[L])$; $K_{A,h} = ([H][H_{h-1}L])/[H_hL]$. [b] NMR titration, no control of ionic strength, NaOH/HCl/D_2O for pH adjustment.

Table 3. Stability constants $\log\beta_{hlm}$[a] of complexes of H_6L^1, H_5L^2 and H_5dtpa with divalent metal ions and corresponding dissociation constants $pK_{A,hlm}$[a] (I = 0.1 M NMe_4Cl, 25 °C, unless stated otherwise). Metal-coordinated water molecules are omitted for clarity.

Equilibrium		Cu^{2+}			Zn^{2+}			Ca^{2+}		
		H_6L^1	H_5L^2	H_5dtpa[b]	H_6L^1	H_5L^2	H_5dtpa[b]	H_6L^1	H_5L^2	H_5dtpa[b]
		$\log\beta_{hlm}$								
$M^{2+} + L^{n-} \rightleftharpoons [M(L)]^{(n-2)-}$	$\log\beta_{011}$	21.43(6)	19.47(4)	21.2	19.67(6)	18.18(3)	18.2	10.70(4)	9.38(2)	10.75
$M^{2+} + L^{n-} + H^+ \rightleftharpoons [M(HL)]^{(n-3)-}$	$\log\beta_{111}$	28.29(5)	23.30(3)	26.00	26.92(5)	22.15(2)	23.80	18.27(2)	15.48(5)	16.86
$M^{2+} + L^{n-} + 2H^+ \rightleftharpoons [M(H_2L)]^{(n-4)-}$	$\log\beta_{211}$	31.95(3)	25.90(3)	28.96	30.65(2)	24.32(1)	–	23.83(8)	21.03(4)	–
$M^{2+} + L^{n-} + 3H^+ \rightleftharpoons [M(H_3L)]^{(n-5)-}$	$\log\beta_{311}$	34.41(4)	–	–	32.82(3)	25.69(8)	–	–	24.06(4)	–
$2M^{2+} + L^{n-} + 2H_2O \rightleftharpoons [M_2(OH)_2(L)]^{(n-2)-} + 2H^+$	$\log\beta_{-212}$	11.02(7)	8.25(5)	–	7.43(9)	5.10(4)	–	–	–	–
$2M^{2+} + L^{n-} + H_2O \rightleftharpoons [M_2(OH)(L)]^{(n-3)-} + H^+$	$\log\beta_{-112}$	20.41(7)	16.46(7)	–	16.2(1)	–	–	–	–	–
$2M^{2+} + L^{n-} \rightleftharpoons [M_2(L)]^{(n-4)-}$	$\log\beta_{012}$	28.15(7)	24.10(4)	–	25.10(9)	20.81(8)	–	13.23(8)	11.62(8)	–
$2M^{2+} + L^{n-} + H^+ \rightleftharpoons [M_2(HL)]^{(n-5)-}$	$\log\beta_{112}$	32.60(4)	–	–	–	–	–	–	–	–
		$pK_{A,hlm}$								
$[M(HL)]^{(n-3)-} \rightleftharpoons [M(L)]^{(n-2)-} + H^+$		6.86	3.83	4.80	7.24	3.97	5.60	7.57	6.10	6.11
$[M(H_2L)]^{(n-4)-} \rightleftharpoons [M(HL)]^{(n-3)-} + H^+$		3.66	2.60	2.96	3.74	2.17	–	5.56	5.55	–
$[M(H_3L)]^{(n-5)-} \rightleftharpoons [M(H_2L)]^{(n-4)-} + H^+$		2.46	–	–	2.16	1.37	–	–	3.03	–
$[M_2(OH)(L)]^{(n-3)-} + H_2O \rightleftharpoons [M_2(OH)_2(L)]^{(n-2)-} + H^+$		9.39	8.21	–	8.81	*7.86*[c]	–	–	–	–
$[M_2(L)]^{(n-4)-} + H_2O \rightleftharpoons [M_2(OH)(L)]^{(n-3)-} + H^+$		7.74	7.64	–	8.86	*7.86*[c]	–	–	–	–
$[M_2(HL)]^{(n-5)-} \rightleftharpoons [M_2(L)]^{(n-4)-} + H^+$		4.45	–	–	–	–	–	–	–	–

[a] $\beta_{hlm} = [H_hL_lM_m]/([H]^h[L]^l[M]^m)$; $K_{A,hlm} = ([H][H_{h-1}L_lM_m])/[H_hL_lM_m]$. [b] Ref.[25], 0.1 M K^+ salts as background electrolytes. [c] Simultaneous dissociation of two protons.

Table 4. Stability constants $\log\beta_{hlm}$[a] of complexes of H_6L^1, H_5L^2 and H_5dtpa with trivalent metal ions La^{3+}, Eu^{3+} and Gd^{3+} and corresponding dissociation constants $pK_{A,hlm}$[a] (I = 0.1 M NMe_4Cl, 25 °C, unless stated otherwise). Metal-coordinated water molecules are omitted for clarity.

Equilibrium		La^{3+}			Eu^{3+}			Gd^{3+}		
		H_6L^1	H_5L^2	H_5dtpa[b]	H_6L^1	H_5L^2	H_5dtpa[b]	H_6L^1	H_5L^2	H_5dtpa[b]
		$\log\beta_{hlm}$								
$M^{3+} + L^{n-} \rightleftharpoons [M(L)]^{(n-3)-}$	$\log\beta_{011}$	20.54(8)	17.54(2)	19.5	22.36(3)	19.82(1)	22.4	22.34(2)	19.47(2)	22.2[c]
$M^{3+} + L^{n-} + H^+ \rightleftharpoons [M(HL)]^{(n-4)-}$	$\log\beta_{111}$	26.25(5)	20.44(5)	21.1	28.75(1)	22.23(1)	24.6	28.82(1)	22.01(2)	24.6
$M^{3+} + L^{n-} + 2H^+ \rightleftharpoons [M(H_2L)]^{(n-5)-}$	$\log\beta_{211}$	29.43(3)	22.86(7)	–	31.07(1)	23.52(8)	–	31.17(1)	23.4(1)	
$M^{3+} + L^{n-} + 3H^+ \rightleftharpoons [M(H_3L)]^{(n-6)-}$	$\log\beta_{311}$	–	25.26(6)	–	–	–	–	–	–	
$2M^{3+} + L^{n-} + 2H_2O \rightleftharpoons [M_2(OH)_2(L)]^{(n-4)-} + 2H^+$	$\log\beta_{-212}$	7.3(2)	3.45(4)	–	10.94(6)	7.39(6)	–	11.53(7)	7.29(6)	
$2M^{3+} + L^{n-} + H_2O \rightleftharpoons [M_2(OH)(L)]^{(n-5)-} + H^+$	$\log\beta_{-112}$	17.2(2)	–	–	20.04(6)	–	–	20.46(8)	–	
$2M^{3+} + L^{n-} \rightleftharpoons [M_2(L)]^{(n-6)-}$	$\log\beta_{012}$	25.2(2)	–	–	27.53(5)	–	–	27.92(5)	22.10(9)	
$2M^{3+} + L^{n-} + H^+ \rightleftharpoons [M_2(HL)]^{(n-7)-}$	$\log\beta_{112}$	–	–	–	–	–	–	31.05(8)	–	
		$pK_{A,hlm}$								
$[M(HL)]^{(n-4)-} \rightleftharpoons [M(L)]^{(n-3)-} + H^+$		5.70	2.99	2.6	6.39	2.41	2.2	6.48	2.54	2.4
$[M(H_2L)]^{(n-5)-} \rightleftharpoons [M(HL)]^{(n-4)-} + H^+$		3.18	2.42	–	2.32	1.29	–	2.34	1.41	
$[M(H_3L)]^{(n-6)-} \rightleftharpoons [M(H_2L)]^{(n-5)-} + H^+$		–	2.40	–	–	–	–	–	–	–
$[M_2(OH)(L)]^{(n-5)-} + H_2O \rightleftharpoons [M_2(OH)_2(L)]^{(n-4)-} + H^+$		9.9	–	–	9.10	–	–	8.92	*7.41*[d]	–
$[M_2(L)]^{(n-6)-} + H_2O \rightleftharpoons [M_2(OH)(L)]^{(n-5)-} + H^+$		8.1	–	–	7.49	–	–	7.46	*7.41*[d]	–
$[M_2(HL)]^{(n-7)-} \rightleftharpoons [M_2(L)]^{(n-6)-} + H^+$		–	–	–	–	–	–	3.14	–	–

[a] $\beta_{hlm} = [H_hL_lM_m]/([H]^h[L]^l[M]^m)$; $K_{A,hlm} = ([H][H_{h-1}L_lM_m])/[H_hL_lM_m]$. [b] Ref.[25], 0.1 M K^+ salts as background electrolytes. [c] Ref.[22] [d] Simultaneous dissociation of two protons.

metal ion to these ligands is probably analogous. Therefore, one can suggest that both metal ions in the dinuclear complexes are coordinated separately by the opposite H_2ida-like sides of ligands and behave almost independently. The stabilities of these dinuclear complexes with transition-metal ions are comparable in the cases of H_6L^1 and H_5dtpa, but corresponding complexes of the phosphinate ligand are much less stable. However, stability of calcium(II) dinuclear complexes is comparable in all the cases (Table 6). Representative distribution diagrams of copper(II)/ligand systems are shown in Figures S2 and S3 (see Supporting Information).

Lanthanide(III) ions are usually fully encapsulated in eight coordinating atoms of H_5dtpa-like ligands. This coordination mode was also proved in the case of these phosphorus-containing ligands.[16] Therefore, protonations of their complexes occurs on non-coordinated oxygen atoms of the coordinated pendant moieties. In the case of the phosphonic ligand, first pK_A's are in range 5.70–6.48, which corresponds to the deprotonation of the coordinated

Table 5. Stability constants $\log\beta_{hlm}$[a] of complexes of H_6L^1, H_5L^2 and H_5dtpa with the trivalent metal ions Lu^{3+} and $Y^{3+}$and corresponding dissociation constants $pK_{A,hlm}$[a] (I = 0.1 M NMe_4Cl, 25 °C, unless stated otherwise). Metal-coordinated water molecules are omitted for clarity.

Equilibrium		Lu^{3+} H_6L^1	H_5L^2	H_5dtpa[b]	Y^{3+} H_6L^1	H_5L^2	H_5dtpa[b]
		$\log\beta_{hlm}$					
$M^{3+} + L^{n-} \leftrightharpoons [M(L)]^{(n-3)-}$	$\log\beta_{011}$	21.82(4)	19.35(3)	22.5	21.16(2)	18.80(3)	22.5[c]
$M^{3+} + L^{n-} + H^+ \leftrightharpoons [M(HL)]^{(n-4)-}$	$\log\beta_{111}$	27.85(2)	21.81(3)	24.7	27.52(1)	21.30(4)	24.4
$M^{3+} + L^{n-} + 2H^+ \leftrightharpoons [M(H_2L)]^{(n-5)-}$	$\log\beta_{211}$	30.27(3)	23.79(5)	–	30.18(1)	23.34(7)	
$M^{3+} + L^{n-} + 3H^+ \leftrightharpoons [M(H_3L)]^{(n-6)-}$	$\log\beta_{311}$	32.11(5)	–	–	–	–	–
$2M^{3+} + L^{n-} + 2H_2O \leftrightharpoons [M_2(OH)_2(L)]^{(n-4)-} + 2H^+$	$\log\beta_{-212}$	11.99(8)	8.28(6)	–	–	6.7(1)	–
$2M^{3+} + L^{n-} + H_2O \leftrightharpoons [M_2(OH)(L)]^{(n-5)-} + H^+$	$\log\beta_{-112}$	20.05(8)	–	–	16.48(4)	–	–
$2M^{3+} + L^{n-} \leftrightharpoons [M_2(L)]^{(n-6)-}$	$\log\beta_{012}$	26.74(7)	–	–	–	–	–
$2M^{3+} + L^{n-} + H^+ \leftrightharpoons [M_2(HL)]^{(n-7)-}$	$\log\beta_{112}$	30.42(6)	–	–	–	–	–
		$pK_{A,hlm}$					
$[M(HL)]^{(n-4)-} \leftrightharpoons [M(L)]^{(n-3)-} + H^+$		6.04	2.46	2.2	6.36	2.50	1.9
$[M(H_2L)]^{(n-5)-} \leftrightharpoons [M(HL)]^{(n-4)-} + H^+$		2.41	1.98	–	2.66	2.04	–
$[M(H_3L)]^{(n-6)-} \leftrightharpoons [M(H_2L)]^{(n-5)-} + H^+$		1.84	–	–	–	–	–
$[M_2(OH)(L)]^{(n-5)-} + H_2O \leftrightharpoons [M_2(OH)_2(L)]^{(n-4)-} + H^+$		8.05	–	–	–	–	–
$[M_2(L)]^{(n-6)-} + H_2O \leftrightharpoons [M_2(OH)(L)]^{(n-5)-} + H^+$		6.69	–	–	–	–	–
$[M_2(HL)]^{(n-7)-} \leftrightharpoons [M_2(L)]^{(n-6)-} + H^+$		3.68	–	–	–	–	–

[a] $\beta_{hlm} = [H_hL_lM_m]/([H]^h[L]^l[M]^m)$; $K_{A,hlm} = ([H][H_{h-1}L_lM_m])/[H_hL_lM_m]$. [b] Ref.[25], 0.1 M K^+ salts as background electrolytes. [c] Ref.[22]

Table 6. Stability constants of dinuclear complexes $[M_2L]$ of H_6L^1, H_5L^2 and H_5dtpa and the complex [ML] of H_2ida with selected metal ions (I = 0.1 M NMe_4Cl, 25 °C, unless stated otherwise).

Ligand	$\log K$[a] Cu^{2+}	Zn^{2+}	Ca^{2+}	La^{3+}	Eu^{3+}	Gd^{3+}	Lu^{3+}
H_6L^1	6.72	5.43	2.53	4.7	5.17	5.58	4.92
H_5L^2	4.63	2.63	2.24	–	–	2.63	–
H_5dtpa[b]	6.79	4.48	1.6	–	3.2	–	–
H_2ida[b,c]	10.56	7.15	2.60	5.88	6.73	6.68	7.61

[a] $K = [M_2L]/([M][ML])$ for H_6L^1, H_5L^2 and H_5dtpa and $K = [ML]/([M][L])$ for H_2ida. [b] Ref.[25], 0.1 M K^+ salts as background electrolytes. [c] H_2ida = iminodiacetic acid.

phosphonate arm. Second protonations occur with pK_A's in the range 2.3–3.2, comparable to that reported for complexes of H_5dtpa (1.9–2.6) and take place on carboxylate moieties. The phosphonate ligand forms relatively stable dinuclear complexes, which is probably a consequence of the high charge of the deprotonated phosphonate and its ability to bridge coordination polyhedrons (Table 6). Contrary, dinuclear complexes of the phenylphosphinate ligand and H_5dtpa itself are much less stable and were detected only in few cases due to a precipitation of metal hydroxides, which occurred in the other systems.

Representative distribution diagrams of gadolinium(III)/ligand systems are shown in Figure 2 and Figure 3. In the 1:1 mixtures, the Gd^{3+} ion is fully encapsulated to the complexes above pH 3. Comparing the distributions simulated for twofold excess of the metal ion, the phosphonate ligand binds second Gd^{3+} ion much better than the phosphinate, as a result of the higher negative charge of the ligand and the better possibility of the phosphonate to serve as a bridging group in the binuclear complexes (see parts B in Figures 2 and 3). Relatively high concentration of the free Gd^{3+} ion in Figure 3 (B) at high pH values is not reasonable, and it is a result of the conditions used for the simulation. In

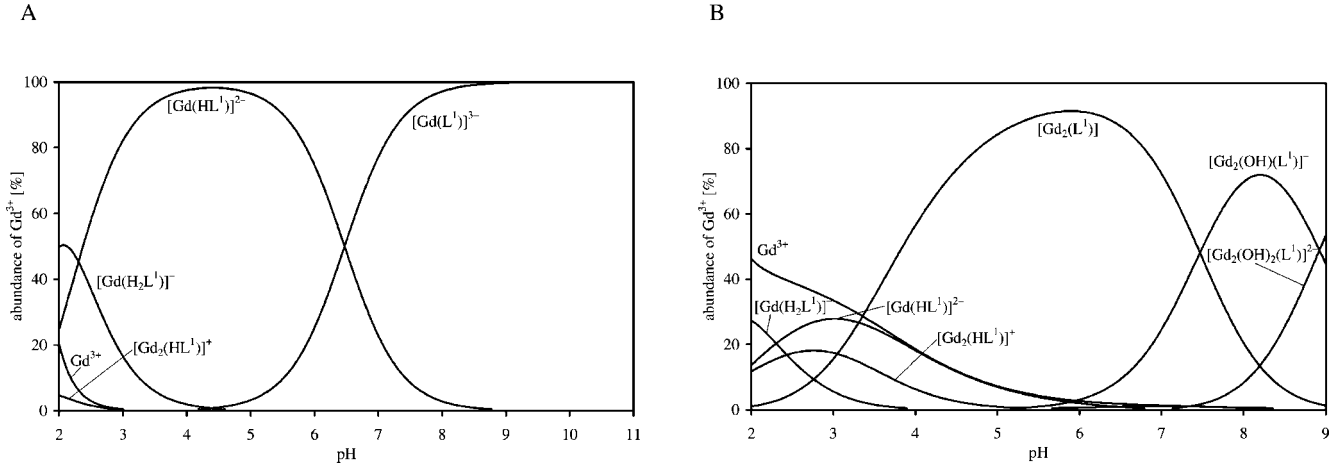

Figure 2. Distribution diagrams of H_6L^1/Gd^{3+} systems in (A) 1:1 and (B) 1:2 ratios [$c(H_6L^1)$ = 0.004 M].

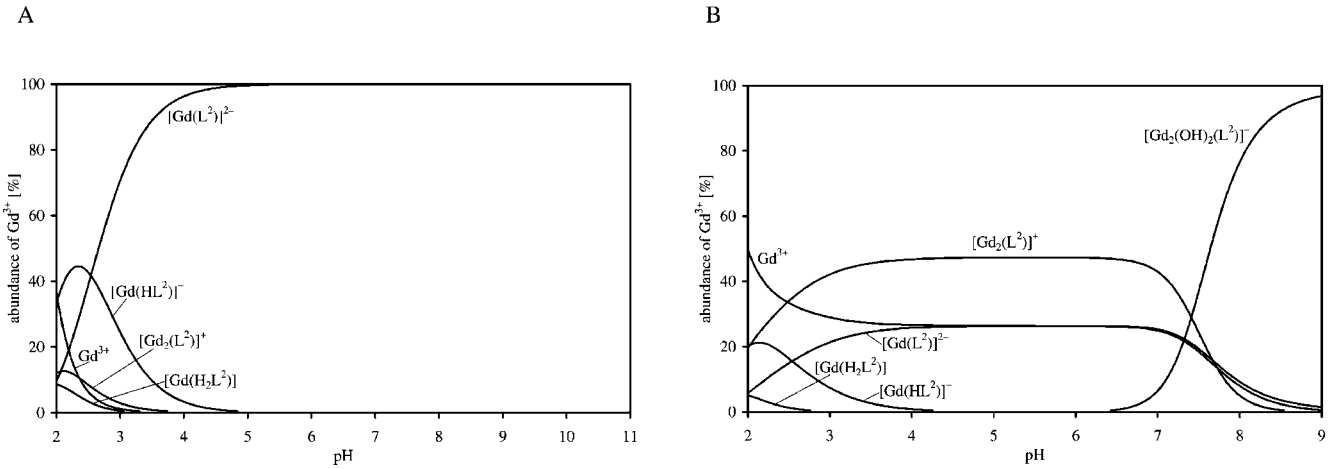

Figure 3. Distribution diagrams of H_5L^2/Gd^{3+} systems in (A) 1:1 and (B) 1:2 ratios [$c(H_5L^2)$ = 0.004 M].

the real titration of H_5L^2/Ln^{3+} systems, only 1.5-fold excess of hydrolyzable Ln^{3+} ions was used and, therefore, the concentration of the free metal ions was suppressed.

Comparison of the determined stability constants of phosphorus acid derivatives with those found for H_5dtpa and H_2ida shows differences. The stability constants in H_2ida series follow the expected trend and increase from lanthanum(III) to lutetium(III). For H_5dtpa, the values increase from La^{III} to Eu^{III} and then are similar to the end of lanthanide series. For the phosphorus acid derivatives, the highest values were found for Eu^{III} and Gd^{III}, and then decrease to Lu^{III} and Y^{III}. These results indicate that size of the coordination cavity of H_5dtpa and its phosphorus acid derivatives is optimal for ions in the middle of lanthanide series. In contrast to the H_5dtpa, in the new ligands the phosphorus groups are too large and the ligands form bigger cavity which do not fit to the heavy lanthanides(III) or yttrium(III).

Dissociation Kinetics

In preliminary experiments, the gadolinium(III) complexes with the new ligands were found to be much less stable against proton- and metal-assisted dissociations, comparing to the gadolinium(III) complex of H_5dtpa[26] and its mono- and bis-amides.[27,28] Therefore, the kinetic data had to be acquired by a stopped-flow technique. Dissociation reactions were performed in high excess (10–70×) of the concurrent metal ion (Cu^{2+} or Eu^{3+}), ensuring pseudo-first-order reaction conditions, and in buffered solutions (pH in range 3.5–5.7). The dependences of the observed pseudo-first-order rate constants on the acidity of the solutions are shown in Figure 4, together with the best fits of the experimental data (for discussion of fittings see below).

For decomplexation of the gadolinium(III) complexes of H_5dtpa-like ligands, the general reaction Scheme is usually accepted,[26] where proton and metal-assisted pathways are taking place as shown in Scheme 2.

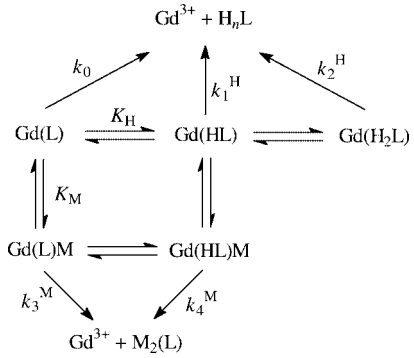

Scheme 2. Reaction mechanism of the dissociation of gadolinium(III) complexes of H_5dtpa-like ligands (charges are omitted for clarity).

Rearrangement of the corresponding rate law gives dependence of pseudo-first order constant $k_{obsd.}$ on proton and concurrent metal ion concentrations as given in Equation (1), similarly as it was evaluated for the fitting of dissociation kinetics of the $[Gd(dtpa)]^{2-}$ complex.[26] Here, the constants K_H and K_M are the protonation constant of the gadolinium(III) complex [Gd(HL)] and the stability constant for the mixed dinuclear gadolinium(III)-attacking metal-ion complex [Gd(L)M], respectively. The protonation and stability constants of $[Gd(H_2L)]$ and [Gd(HL)M] can be omitted from the denominator as the concentration of these complexes is negligible (the values of the corresponding constants are low).

$$k_{obsd.} = \frac{k_0 + k_1^H[H^+] + k_2^H[H^+]^2 + k_3^M[M^{n+}] + k_4^M[H^+][M^{n+}]}{1 + K_H[H^+] + K_M[M^{n+}]} \quad (1)$$

As k_1^H and k_2^H are independent of the nature of concurrent metal ion, the dissociation kinetics for copper(II) and europium(III) systems with the same starting gadolinium(III) complex were fitted simultaneously keeping these parameters identical in both cases. The results of these fittings are

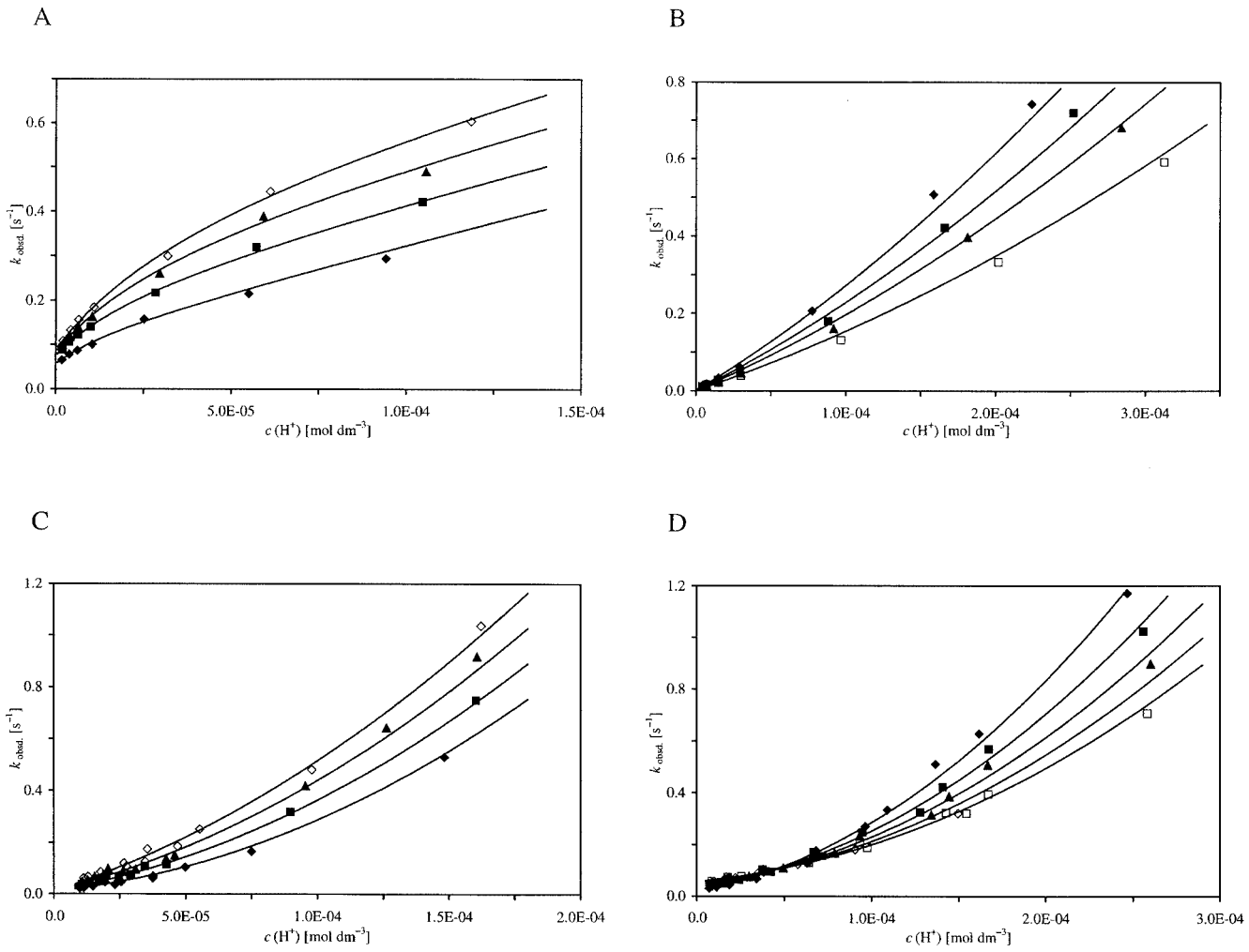

Figure 4. Dependence of pseudo-first-order rate constant $k_{obsd.}$ on proton and metal ion concentrations. Excess of the concurrent metal ion: 10×: full diamond; 20×: full square; 30×: full triangle; 40×: open diamond; 50×: open square; (A) $[Gd(L^1)]^{3-}/Cu^{2+}$ system, (B) $[Gd(L^1)]^{3-}/Eu^{3+}$ system, (C) $[Gd(L^2)]^{2-}/Cu^{2+}$ system, (D) $[Gd(L^2)]^{2-}/Eu^{3+}$ system.

compiled in Table 7 and the representative fits of the pH-dependence of the first-order rate constants $k_{obsd.}$ are shown in Figure 4.

As the pH region where dissociations were studied is much lower (3.5–5.7) than the pK_A of the $[Gd(HL^1)]^{2-}$ complex (6.5, Table 4), one can suggest that the singly protonated complex species $[Gd(HL^1)]^{2-}$ is the major species in the reacting solution (Figure 2). Therefore, the calculated constant K_H corresponds to the second protonation of the complex species. This hypothesis can be supported by the relatively low value of this constant (the corresponding pK_A is 3.7, Table 7).

In the case of the copper(II)-assisted dissociation of the $[Gd(L^1)]^{3-}$ complex (Figure 4, A), the most complicated rate

Table 7. Rate and equilibrium constants characterizing the dissociation reactions between the complexes $[Gd(L^1)]^{3-}$, $[Gd(L^2)]^{2-}$ and $[Gd(dtpa)]^{2-}$, and Cu^{2+} and Eu^{3+} ions (25 °C, 1.0 M KCl).

Constant	Complex $[Gd(L^1)]^{3-}$	$[Gd(L^2)]^{2-}$	$[Gd(dtpa)]^{2-}$ [a]
k_1^H [M^{-1} s^{-1}]	$(3.38 \pm 0.22) \times 10^3$	$(1.57 \pm 0.18) \times 10^3$	0.58
k_2^H [M^{-2} s^{-1}]	$(1.02 \pm 0.20) \times 10^7$	$(1.51 \pm 0.11) \times 10^7$	$9.7 \cdot 10^4$
k_3^{Cu} [M^{-1} s^{-1}]	33 ± 3	–	0.93
k_4^{Cu} [M^{-2} s^{-1}]	$(9.4 \pm 1.3) \times 10^5$	$(5.4 \pm 0.3) \times 10^5$	–
K_{Cu} [M^{-1}]	–	–	13
k_3^{Eu} [M^{-1} s^{-1}]	–	2.2 ± 0.5	$4.9 \cdot 10^{-4}$
k_4^{Eu} [M^{-2} s^{-1}]	–	–	40
K_{Eu} [M^{-1}]	50 ± 7	20.0 ± 2.3	20
K_H [M^{-1}]	$(5.7 \pm 0.8) \times 10^3$	–	100

[a] Ref.[26]

law was found. The best fits were obtained according to Equation (2) which is formally derived from Equation (1) when the term $K_M[Cu^{2+}]$ in the denominator is neglected, as can be because the K_M value is low, comparing to the value of the protonation constant K_H. The reaction rate increases with both proton and copper(II) concentrations, and a saturation-like shape of $k_{obsd.}$ dependences (Figure 4, A) reveals a formation of the protonated complex, which slightly slow down the dissociation reaction as the Cu^{2+} ion cannot easily attack the less negatively charged protonated complex $[Gd(H_2L^1)]^-$ in comparison with $[Gd(HL^1)]^{2-}$.

$$k_{obsd.} = \frac{k_1^H[H^+] + k_2^H[H^+]^2 + k_3^{Cu}[Cu^{2+}] + k_4^{Cu}[H^+][Cu^{2+}]}{1 + K_H[H^+]} \quad (2)$$

However, in the europium(III)-promoted dissociation of $[Gd(L^1)]^{3-}$ complex, only proton-assisted pathways were found, as the observed rate constant $k_{obsd.}$ can be extrapolated to zero at zero proton concentration. Furthermore, the increase in the Eu^{3+} concentration dropped the value of $k_{obsd.}$ (Figure 4, B), which is an evidence for the formation of a dinuclear complex. This complex is kinetically relatively stable, and its structure should be analogous to the dinuclear $[Gd_2(L^1)]$ species (Figure 2, B). The presence of the highly charged metal ions bound on opposite sides of the complex prevents the attack by an additional proton. Therefore, the data were best fitted according to Equation (3).

$$k_{obsd.} = \frac{k_1^H[H^+] + k_2^H[H^+]^2}{1 + K_{Eu}[Eu^{3+}]} \quad (3)$$

The copper(II)-assisted dissociation of the $[Gd(L^2)]^{2-}$ complex can be best fitted by Equation (4), which can be derived from Equation (1) by neglecting of the stabilization of the gadolinium(III) complex by the protonated and dinuclear species formation [i.e. $1 >> K_H[H^+] + K_M[Cu^{2+}]$ in the denominator of Equation (1)], as the stability of the dinuclear complex with Cu^{2+} is even lower for the phosphinate derivative H_5L^2 comparing to phosphonate ligand H_6L^1 and also because of the lower protonation constants of the $[Gd(L^2)]^{2-}$ complex the term $K_H[H^+]$ is of a low importance. The representative data are given together with the best fits in Figure 4 (C).

$$k_{obsd.} = k_1^H[H^+] + k_2^H[H^+]^2 + k_4^{Cu}[H^+][Cu^{2+}] \quad (4)$$

In the case of the europium(III)-assisted dissociation of the $[Gd(L^2)]^{2-}$ complex, the crossing region in $k_{obsd.}$ dependences on the proton concentration was found at $[H^+]$ of about $5 \cdot 10^{-5}$ M (pH ≈ 4.3, Figure 4, D). At higher proton concentrations, the increase in Eu^{3+} concentration slows down the reaction rate, contrary, at low proton concentrations, the reaction accelerates with increasing Eu^{3+} concentration. Similar behaviour was reported for the Eu^{3+}-promoted dissociation of the $[Gd(dtpa)]^{2-}$ complex.[26] The non-zero reaction rate at the zero proton concentration is an evidence for the proton-independent term in the rate law. Therefore, the best fits were obtained using Equation (5).

$$k_{obsd.} = \frac{k_1^H[H^+] + k_2^H[H^+]^2 + k_3^{Eu}[Eu^{3+}]}{1 + K_{Eu}[Eu^{3+}]} \quad (5)$$

Spontaneous dissociation of diprotonated complex $[Gd(H_2L^1)]^-$ and the monoprotonated complexes $[Gd(HL^2)]^-$ is about three orders in magnitude faster than in the case of $[Gd(Hdtpa)]^-$ complex (Table 7). Further protonation causes noticeable increase in the reaction rate of about four orders in all the cases.

To compare the kinetic inertness of the complex species with the new ligands and that with H_5dtpa, we calculated half-life times of all the complex species under various conditions (Table 8).

Table 8. Comparison of half-life times of the complexes $[Gd(L^1)]^{3-}$, $[Gd(L^2)]^{2-}$ and $[Gd(dtpa)]^{2-}$ in various reaction media (25 °C, I = 1.0 M KCl).

Conditions	Half-life times [s] $[Gd(L^1)]^{3-}$	$[Gd(L^2)]^{2-}$	$[Gd(dtpa)]^{2-}$
	pH = 4.0		
without metal ions	2.5	2.2	680
0.001 M Cu^{2+}	1.9	1.9	360
0.001 M Eu^{3+}	2.6	2.3	690
0.01 M Cu^{2+}	0.6	0.8	77
0.01 M Eu^{3+}	3.3	2.5	780
	pH = 5.0		
without metal ions	21	40	$4.5 \cdot 10^4$
0.001 M Cu^{2+}	9.5	31	740
0.001 M Eu^{3+}	22	37	$4.3 \cdot 10^4$
0.01 M Cu^{2+}	1.6	9.7	84
0.01 M Eu^{3+}	31	21	$3.4 \cdot 10^4$
	pH = 6.0		
without metal ions	210	440	$1.0 \cdot 10^6$
0.001 M Cu^{2+}	19	330	750
0.001 M Eu^{3+}	220	190	$5.8 \cdot 10^5$
0.01 M Cu^{2+}	2.0	99	84
0.01 M Eu^{3+}	310	35	$1.4 \cdot 10^5$

In general, the stability of the complexes of new phosphorus-containing ligands is much lower comparing to that of $[Gd(dtpa)]^{2-}$. Increase in copper(II) concentration speed-up the dissociation reaction in all the cases, bud especially, for $[Gd(dtpa)]^{2-}$ complex in neutral solutions, where is the half-life time comparable to that calculated for $[Gd(L^2)]^{2-}$. It is a consequence of a spontaneous dissociation of dinuclear [Gd(dtpa)Cu] complex. In the case of $[Gd(L^2)]^{2-}$, the lower basicity of the donor groups results in lower ability of binuclear complex formation (see also the values of stability constants of dinuclear species, Table 6) and therefore, to worse formation of such reactive intermediate. For europium(III)-promoted dissociations, the stabilization of [Gd(L)] complexes with increasing Eu^{3+} concentration was found in all the cases at low pH. It is the result of formation of [Gd(L)Eu] complexes, which cannot be easily attacked by

proton and their own dissociation is slower comparing to proton-assisted pathway. Increasing the pH, half-life times slightly drop with increasing Eu^{3+} concentration for $[Gd(dtpa)]^{2-}$ and $[Gd(L^2)]^{2-}$ complexes, as result of their spontaneous dissociation. However, in the case of $[Gd(L^1)Eu]$, there was no evidence for such process and therefore, half-life times still increase.

For the H_5dtpa and its various amide derivatives, all the gadolinium(III) complexes have similar kinetic stability comparing to each other.[26–28] Surprisingly, we found that the gadolinium(III) complexes with H_5dtpa-analogues derived on the central nitrogen atom by the phosphorus acid pendant arm are much less kinetically stable with the half-life times about two to three orders of magnitude shorter. This can probably be attributed to a steric strain in the new complexes, which coordination sphere is not so compact and which can be attacked by a proton or by an additional metal ion. Furthermore, the complex of phosphonate ligand can easily be protonated due to the high basicity of the pendant arm. Also, it can easily form dinuclear complexes, which are the intermediates in the dissociation mechanism. Anyway, the rate constants for complexes of both ligands with phosphorus pendant arm are comparable, so the stereochemistry of both the complexes and the intermediates is probably similar. It should be noticed that assistance of proton or the metal ions in the decomplexation is much more pronounced for H_5dtpa complex itself. The results obtained here correspond very well with *trans*-chelation experiments between the gadolinium(III) complexes and Zn^{2+} followed by ^1H relaxation measurements (Gd^{3+} complex/Zn^{2+} = 1:1, pH 7, phosphate buffer, 37 °C).[16] The experiments gave the same relative kinetic inertness of the complexes $[Gd(dtpa)]^{2-} >> [Gd(L^1)]^{3-} \approx [Gd(L^2)]^{2-}$. On the other hand, a difference in kinetic inertness (pH 2, 25 °C) of the gadolinium(III) complexes of H_4dota and its monophosphonate analog H_5do3ap are much smaller; the $[Gd(do3ap)]^{2-}$ complex decomposes about one order of magnitude faster ($\tau_{1/2}$ = 7.9 h) than the $[Gd(dota)]^-$ complex ($\tau_{1/2}$ = 95.5 h).[29]

Conclusions

The study of thermodynamic and kinetic stabilities of the complexes of phosphonate and phenylphosphinate analogues of H_5dtpa (derived by phosphorus functionality on the central nitrogen atom) with selected transition and lanthanide metal ions is presented. Both phosphorus-containing ligands form thermodynamically very stable complexes, with stability constants comparable or even higher than those reported for parent H_5dtpa. However, the kinetic stability of their gadolinium(III) complexes against acid- and metal-assisted decomplexations is surprisingly much lower. The half-life times of the gadolinium(III) complexes of the new ligands in the presence of an excess of the concurrent metal ions [copper(II) or europium(III)] are shorter by about 2–3 orders of magnitude comparing to those of H_5dtpa and its amidic derivatives. This can probably be attributed to the steric strain in the new complexes, to a high affinity of the phosphonate ligand for protons and/or to the easy formation of binuclear complexes, which acts as the intermediates in the dissociation mechanism. The data presented here show that lanthanide(III) complexes of this class of ligands are less suitable for medicinal use due to the rather low kinetic inertness.

Experimental Section

Materials: The ligands used in this work were prepared according to reported procedures.[16] Metal salts were of analytical grade and were used as obtained from commercial sources or after recrystallization from water. The deionized water (Milli-Q, Millipore, 20 kΩ) was used for physico-chemical experiments. Materials (analytical grade) for preparation of the buffer solutions were obtained from commercial sources.

Equilibrium Studies

The stock solution of hydrochloric acid (ca. 0.03 mol·dm^{-3}) was prepared from 35% aqueous solution (quality "puriss.", Fluka). Commercial NMe_4Cl (99%, Fluka) was recrystallized from boiling *i*PrOH and the solid salt was dried with P_2O_5 in vacuo to constant weight (this dried form of the salt is extremely hygroscopic).[29] Carbonate-free NMe_4OH solution (ca. 0.2 mol·dm^{-3}) was prepared from NMe_4Cl using ion exchanger Dowex 1 in the OH^- form (elution with carbonate-free water, under argon). The hydroxide solution was standardized against potassium hydrogen phthalate and the HCl solution against the ca. 0.2 mol·dm^{-3} NMe_4OH solution.

The ligand stock solutions ($c \approx 0.02$ mol·dm^{-3}) were prepared by dissolution of a weighted amount of the solid hydrochloride salts of ligands (H_6L^1·HCl·2H_2O and H_5L^2·2HCl·H_2O, respectively) in an appropriate amount of deionized water. The exact content of hydrochloric acid was determined gravimetrically as AgCl. Concentrations of the ligands were calculated from potentiometrical data during the determination of the protonation constants using the OPIUM program package.[30] The exact concentrations of metal chlorides stock solutions were determined by titrations with standardized solution of Na_2H_2edta.

Titrations were carried out in a vessel thermostatted at 25 ± 0.1 °C, at an ionic strength $I(NMe_4Cl)$ = 0.1 mol·dm^{-3} and in the presence of extra HCl in the $-\log[H^+]$ range 1.5–12.0 (except of titrations in presence of excess of hydrolyzing metal ions, which were finished at $-\log[H^+]$ of about 9.5) using a PHM 240 pH meter, 2-mL ABU 900 automatic piston burette and a GK 2401B combined electrode (Radiometer). The initial volume of the measured solution was about 5 cm^3 and concentrations of ligands were about 0.004 mol·dm^{-3}. For determination of the stability constants of metal complexes, the mixtures with one or 1.5–2 equivalents of metal ions were used. Titration of each system in each M:L ratio was carried out at least three times and each titration consisted of about 40 data points. An inert atmosphere was ensured by constant flow of dinitrogen saturated with the water vapour by passing through 0.1 mol·dm^{-3} solution of NMe_4Cl. The concentration protonation constants β_h are defined by the equation

$$\beta_h = [H_hL]/([H]^h[L])$$

As dissociation constant $K_{A,h}$ is commonly defined by

$$K_{A,h} = ([H][H_{h-1}L])/[H_hL],$$

it is evident, that $pK_{A,h} = \log\beta_h - \log\beta_{h-1}$.

The concentration stability constants β_{hlm} are defined by the equation

$\beta_{hlm} = [H_hL_lM_m]/([H]^h[L]^l[M]^m)$,

and dissociation constant $K_{A,hlm}$ can be defined similarly to the case of free ligand as

$K_{A,hlm} = ([H][H_{h-1}L_lM_m])/[H_hL_lM_m]$.

Analogously, $pK_{A,hlm} = \log\beta_{hlm} - \log\beta_{h-1lm}$.

The constants (and their standard deviations) were calculated with the OPIUM program package.[30] This program minimizes the criterion of the generalized least-squares method using the calibration function

$E = E_0 + S\times\log[H^+] + j_1\times[H^+] + j_2\times K_w/[H^+]$

where the additive term E_0 contains the standard potentials of the electrodes used and contributions of inert ions to the liquid-junction potential, S corresponds to the Nernstian slope, the value of which should be close to the theoretical value of $RT/zF\{\log(e)\}$ = 59.159 mV. It was reported in the literature that for a glass electrode this value can oscillate at about 99.7% of the theoretical value.[31] The terms $j_1\times[H^+]$ and $j_2\times K_w/[H^+] = j_2\times[OH^-]$ are contributions of H^+ and OH^- ions to the liquid-junction potential. By simple view on the calibration function, it is clear, that they cause a deviation from a linear dependence of E on $[H^+]$ and are significant only in strong acidic and strong alkaline solutions. The calibration parameters were determined from titration of standard HCl with standard NMe_4OH before and immediately after the titration of ligand or ligand-metal system. Thus, two sets of calibration parameters for each titration were used for the calculations of the constants. The water ion product pK_w = 13.81 and the stability constants of hydroxo metal complexes were taken from the literature.[25,32]

Kinetic Studies

The stock solutions of ligands of the concentration of about 0.05 mol·dm^{-3} were prepared by dissolution of a weighted amount of solid hydrochloride salts (H_6L^1·HCl·2H_2O and H_5L^2·2HCl·H_2O, respectively) in appropriate amounts of double-distilled water. Exact content of ligands was determined by addition of a defined excess of $EuCl_3$ and re-titration with a standardized solution of Na_2H_2edta (xylenol orange indicator, pH 5.8–6.0, urotropine buffer). The concentrations of lanthanide(III) chlorides stock solutions were determined by titrations with standardized solution of Na_2H_2edta. From the solutions, the gadolinium(III) complexes [c = 0.2 mmol·dm^{-3} for copper(II)-exchange reaction and 2 mmol·dm^{-3} for europium(III)-exchange reaction, respectively] of each ligand were prepared. Constant ionic strength of potassium chloride (1 mol·dm^{-3}) and buffers [0.02 mol·dm^{-3} boric acid in 0.08 mol·dm^{-3} mannitol for the copper(II)-exchange reaction and 0.02 mol·dm^{-3} *N*-methylpiperazine for the europium(III)-exchange reaction] were used to adjust the pH in the range 3.5–5.7. Large excesses of copper(II) (10–50×) and europium(III) (10–70×) chlorides were employed to assure pseudo-first order conditions of the exchange reactions. All metal-assisted dissociation kinetics experiments were followed spectrophotometrically on a stopped-flow apparatus (Applied Photophisics DX-17MV) at 25 °C at 300 nm [copper(II)-promoted decomplexations], 250 nm [europium(III)-exchange on Gd–H_6L^1 system] and 290 nm [europium(III)-exchange on Gd–H_5L^2 system]. The rate constants $k_{obsd.}$ were determined by fitting of the time-dependence of the absorbance with $A_t = (A_\infty - A_0)e^{-kt} + A_0$ and were reproducible within ±5% in the independent runs. The values of the rate constants used for the fittings were the averages from at least two independent runs using a firmware.

X-ray Measurement

A single crystal of H_6L^1·HCl·1.5H_2O suitable for a diffraction experiment was prepared by slow evaporation of a saturated aqueous solution at room temperature. The colourless block-like crystal was mounted on a glass fibre by silicone fat. Diffraction data were collected using graphite-monochromated Mo-K_α radiation with an Enraf–Nonius KappaCCD diffractometer at 150(1) K [Cryostream Cooler (Oxford Cryosystem)] and analyzed using the HKL DENZO program package (ref.[33]). Cell parameters were determined from all data by the same program package.[33] The structure was solved by direct methods (SIR 97[34]) and refined by full-matrix least-squares techniques (SHELXL97[35]). The used scattering factors for neutral atoms were included in the SHELXL97 program. All non-hydrogen atoms were refined anisotropically. The hydrogen atoms were localized in the difference map of electronic density and refined isotropically. The pertinent crystallographic data are presented in Table 9. CCDC-287906 contains the supplementary crystallographic data for this paper. These data can be obtained free of charge from The Cambridge Crystallographic Data Centre via www.ccdc.cam.ac.uk/data_request/cif.

Table 9. Experimental data for determination of the crystal structure of H_6L^1·HCl·1.5H_2O.

Formula	$C_{13}H_{28}ClN_3O_{12.50}P$
M	492.80
T [K]	150
Crystal dimension, mm	0.25×0.28×0.55
Colour and shape	colourless block
Crystal system	triclinic
Space group	$P\bar{1}$ (No. 2)
a [Å]	8.6219(2)
b [Å]	11.8231(2)
c [Å]	12.0663(3)
α [°]	114.9404(12)
β [°]	96.9488(12)
γ [°]	105.7311(14)
V [Å^3]	1033.78(4)
Z	2
D_c [g cm^{-3}]	1.583
λ [Å]	0.71073
μ [mm^{-1}]	0.333
$F(000)$	518
θ range of data collection [°]	2.63–27.50
Index ranges	$-11 < h < 11$ $-15 < k < 15$ $-15 < l < 15$
Data, restraints, parameters	4735, 0, 390
GOF on F^2	1.025
wR (all data), wR' [$I > 2\sigma(I)$][a]	0.1097, 0.0984
R (all data), R' [$I > 2\sigma(I)$][b]	0.0604, 0.0391
Largest diff. peak and hole [e·Å^{-3}]	0.386, –0.493

[a] $wR = [\Sigma w(F_o^2 - F_c^2)^2/\Sigma w(F_o^2)^2]^{1/2}$, $w = 1/[\sigma^2(F_o^2) + (A\times P)^2 + B\times P]$; where $P = (F_o^2 + 2F_c^2)/3$. [b] $R = \Sigma|F_o - F_c|/\Sigma|F_c|$.

Supporting Information (see footnote on the first page of this article): Table of hydrogen bonds found in the structure of H_6L^1·HCl·1.5H_2O; and distribution diagrams of free H_6L^1, free H_5L^2, and 1:1 and 2:1 copper(II)/ligands (H_6L^1 and H_5L^2) mixtures on pH.

Acknowledgments

We thank Dr. I. Císařová for X-ray data collection and Ms. M. Malíková for help with titration experiments. This work was supported by the Grant Agency of the Czech Republic (No. 203/03/

0168), the FP6-projects EMIL (LSHC-2004-503569) and DiMI (LSHB-CT-2005-512146) and COST D18 are acknowledged. JK thanks the Flemish government for a postdoctoral fellowship (bilateral project between Flanders and the Czech Republic BIL/03/10).

[1] *The Chemistry of Contrast Agents in Medical Magnetic Resonance Imaging* (Eds.: A. E. Merbach, É. Tóth), Wiley, Chichester, U.K., **2001**.
[2] *Topics in Current Chemistry*, vol. 221, Springer, Frankfurt/Main, Germany, **2002**.
[3] P. Caravan, J. J. Ellison, T. J. McMurry, R. B. Lauffer, *Chem. Rev.* **1999**, *99*, 2293–2352.
[4] E. Brücher, *Top. Curr. Chem.* **2002**, *221*, 103–122.
[5] S. Laurent, L. Vander Elst, F. Copoix, R. N. Muller, *Invest. Radiol.* **2001**, *36*, 115–122.
[6] S. Aime, M. Botta, M. Fasano, E. Terreno, *Chem. Soc. Rev.* **1998**, *27*, 19–29.
[7] D. H. Powell, O. M. N. Dhubhghaill, D. Pubanz, L. Helm, Y. S. Lebedev, W. Schlaepfer, A. E. Merbach, *J. Am. Chem. Soc.* **1996**, *118*, 9333–9346.
[8] R. Ruloff, É. Tóth, R. Scopelliti, R. Tripier, H. Handel, A. E. Merbach, *Chem. Commun.* **2002**, 2630–2631.
[9] S. Laus, R. Ruloff, É. Tóth, A. E. Merbach, *Chem. Eur. J.* **2003**, *9*, 3555–3566.
[10] Z. Jászberényi, A. Sour, É. Tóth, M. Benmelouka, A. E. Merbach, *Dalton Trans.* **2005**, 2713–2719.
[11] S. Laus, A. Sour, R. Ruloff, É. Tóth, A. E. Merbach, *Chem. Eur. J.* **2005**, *11*, 3064–3076.
[12] S. Laurent, F. Botteman, L. Vander Elst, R. N. Muller, *Eur. J. Inorg. Chem.* **2004**, 463–468.
[13] L. Burai, É. Tóth, A. Sour, A. E. Merbach, *Inorg. Chem.* **2005**, *44*, 3561–3568.
[14] D. J. Sawyer, J. E. Powell, *Polyhedron* **1989**, *8*, 1425–1430.
[15] Y.-M. Wang, C. H. Lee, G.-C. Liu, R.-S. Sheu, *J. Chem. Soc. Dalton Trans.* **1998**, 4113–4118.
[16] J. Kotek, P. Lebdušková, P. Hermann, L. Vander Elst, R. N. Muller, C. F. G. C. Geraldes, T. Maschmeyer, I. Lukeš, J. A. Peters, *Chem. Eur. J.* **2003**, *9*, 5899–5915.
[17] J. Rudovský, J. Kotek, P. Hermann, I. Lukeš, V. Mainero, S. Aime, *Org. Biomol. Chem.* **2005**, *3*, 112–117.
[18] J. Rudovský, P. Cígler, J. Kotek, P. Hermann, P. Vojtíšek, I. Lukeš, J. A. Peters, L. Vander Elst, R. N. Muller, *Chem. Eur. J.* **2005**, *11*, 2373–2384.
[19] P. Lebdušková, J. Kotek, P. Hermann, L. Vander Elst, R. N. Muller, I. Lukeš, J. A. Peters, *Bioconjugate Chem.* **2004**, *15*, 881–889.
[20] J. Rudovský, P. Hermann, M. Botta, S. Aime, I. Lukeš, *Chem. Commun.* **2005**, 2390–2391.
[21] P. Lebdušková, A. Sour, L. Helm, É. Tóth, J. Kotek, I. Lukeš, A. E. Merbach, *Dalton Trans.*, in press.
[22] K. Kumar, C. A. Chang, L. C. Francesconi, D. D. Dischino, M. F. Malley, J. Z. Gougoutas, M. F. Tweedle, *Inorg. Chem.* **1994**, *33*, 3567–3575.
[23] C. F. G. C. Geraldes, A. M. Urbano, M. C. Alpoim, A. D. Sherry, K.-T. Kuan, R. Rajagopalan, F. Maton, R. N. Muller, *Magn. Reson. Imaging* **1995**, *13*, 401–420.
[24] I. Lukeš, J. Kotek, P. Vojtíšek, P. Hermann, *Coord. Chem. Rev.* **2001**, *216–217*, 287–312.
[25] *NIST Standard Reference Database 46 (Critically Selected Stability Constants of Metal Complexes)*, Version 7.0, **2003**.
[26] L. Sarka, L. Burai, E. Brücher, *Chem. Eur. J.* **2000**, *6*, 719–724.
[27] L. Sarka, L. Burai, R. Király, L. Zékány, E. Brücher, *J. Inorg. Biochem.* **2002**, *91*, 320–326.
[28] Z. Jászberényi, É. Tóth, T. Kálai, R. Király, E. Brücher, A. E. Merbach, K. Hideg, *Dalton Trans.* **2005**, 694–701.
[29] P. Táborský, P. Lubal, J. Havel, J. Kotek, P. Hermann, I. Lukeš, *Collect. Czech. Chem. Commun.* **2005**, *70*, 1909–1942.
[30] M. Kývala, I. Lukeš, CHEMOMETRICS '95, Pardubice, Czech Republic, **1995**, Book of Abstracts, p. 63; M. Kývala, P. Lubal, I. Lukeš, SIMEC '98, Girona, Spain, **1998**, Book of Abstracts, p. 94; available free of charge at: http://www.natur.cuni.cz/~kyvala/opium.html.
[31] D. C. Harris, in: *Quantitative Chemical Analysis*, 3rd ed., W. H. Freeman, New York, **1991**, p. 365.
[32] C. F. Baes Jr, R. E. Mesmer, *The Hydrolysis of Cations*, Wiley, New York, **1976**.
[33] Z. Otwinowski, W. Minor, *HKL Denzo and Scalepack Program Package*, Nonius BV, Delft, **1997**; Z. Otwinowski, W. Minor, *Methods Enzymol.* **1997**, *276*, 307–326.
[34] A. Altomare, M. C. Burla, M. Camalli, G. L. Cascarano, C. Giacovazzo, A. Guagliardi, A. G. G. Moliterni, G. Polidori, R. Spagna, *J. Appl. Crystallogr.* **1999**, *32*, 115–119.
[35] G. M. Sheldrick, *SHELXL97. Program for Crystal Structure Refinement from Diffraction Data*, University of Göttingen. Göttingen, **1997**.

Received: December 14, 2005
Published Online: March 22, 2006

